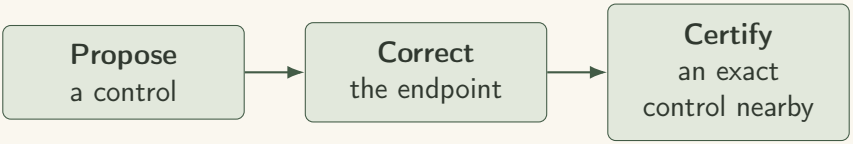
Validated Galerkin Control Reconstruction for Semilinear Wave Equations: Neural–Spectral and Newton–HUM Methods

Tan-Phuc Nguyen Minh-Binh Tran Son Tu

Presented by **Tan-Phuc Nguyen**
Texas A&M University

Nonlinear PDE Seminar

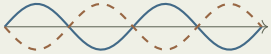


Outline

- **Control Problem and Background**
  Motivation, main problem, and previous works
- **Control Reconstruction**
  Spectral coordinates, learned proposals, and endpoint correction.
- **Validated Guarantees**
  A posteriori certification and source-frozen contraction.
- **Numerical Results and Perspectives**
  Accuracy, computational cost, control effort

Applications of Control Theory

Noise and vibration



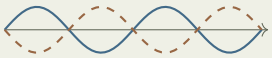
sound + opposing sound

Microphones measure sound; speakers apply a corrective signal.

Control:
Speaker input signal.

Applications of Control Theory

Noise and vibration

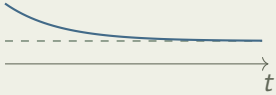


sound + opposing sound

Microphones measure sound; speakers apply a corrective signal.

Control:
Speaker input signal.

Temperature



approach a target

A thermostat uses temperature measurements to adjust heating.

Control:
Heating power.

Applications of Control Theory

Noise and vibration

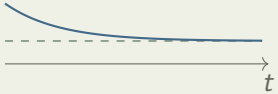


sound + opposing sound

Microphones measure sound; speakers apply a corrective signal.

Control:
Speaker input signal.

Temperature



approach a target

A thermostat uses temperature measurements to adjust heating.

Control:
Heating power.

Energy and transport



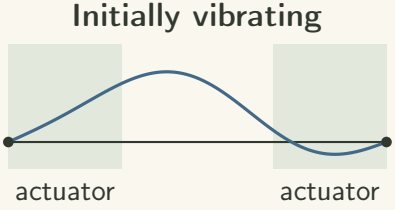
regulate flows on networks

Adjust power or traffic flows under capacity and safety constraints.

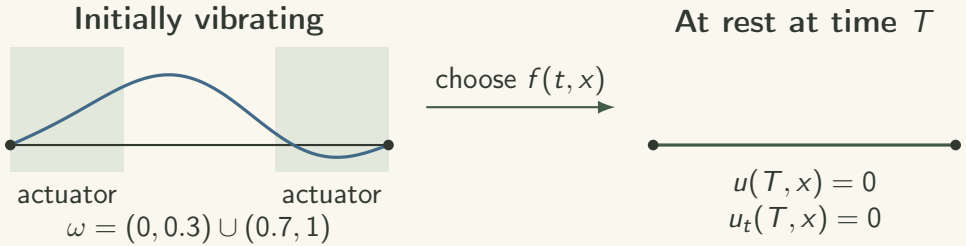
Controls:
Power setpoints;
Traffic-light timings.

What can we measure, what can we change, and how much effort is needed?

Localized Control of Wave Equations



Localized Control of Wave Equations



A flat string is not enough: the velocity must also vanish.

Motivation: From Controllability to Computation

The mathematical question

Can a force applied in just one region make the wave reach a chosen shape and velocity everywhere at a specified time?

Motivation: From Controllability to Computation

The mathematical question

Can a force applied in just one region make the wave reach a chosen shape and velocity everywhere at a specified time?

The computational question

Does this computed control actually steer the system, and what can we prove about it?

Motivation: From Controllability to Computation

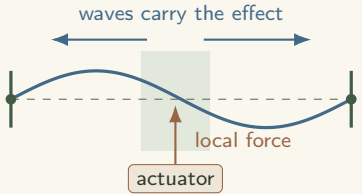
The mathematical question

Can a force applied in just one region make the wave reach a chosen shape and velocity everywhere at a specified time?

The computational question

Does this computed control actually steer the system, and what can we prove about it?

Why do we apply control in just one region?



a vibrating string with fixed ends

Think of stopping a vibrating string.

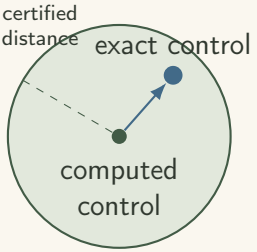
- An actuator acts on a short segment.
- Its effect travels along the string as waves.
- Goal: bring the whole string to rest.

Local force, whole-string target.

Our Main Result: An Exact Control Nearby

From a numerical answer to a guarantee

1. **Compute a candidate.** Use any solver; the result may miss the target slightly.
2. **Check three bounds:** final-state error, correction size, and variation of the final-state response.
3. **Certify an exact control nearby.** If the checks pass, we can find an exact control within a proven distance from our computed control.



▸ Show the theorem

Three validated bounds certify an exact control nearby.

The Semilinear Wave Control Problem

$$\underbrace{u_{tt} - \Delta u}_{\text{wave propagation}} + \underbrace{g(u) + \alpha u}_{\text{internal force}} + \underbrace{f\,\mathbf{1}_{\omega}}_{\text{our control}} = 0, \qquad \alpha \geq 0.$$

The Semilinear Wave Control Problem

$$\underbrace{u_{tt} - \Delta u}_{\text{wave propagation}} + \underbrace{g(u) + \alpha u}_{\text{internal force}} + \underbrace{f\,\mathbf{1}_\omega}_{\text{our control}} = 0, \qquad \alpha \geq 0.$$

Why we introduce Φ? Turn the second-order wave equation into a first-order system.

$$\Phi = (u, u_t) \in \mathcal{E} = H_0^1(\Omega) \times L^2(\Omega), \qquad u|_{\partial\Omega} = 0.$$

The same control problem in state form

$$\begin{cases} \partial_t \Phi + A\Phi + \mathbf{F}\,\mathbf{1}_\omega + G(\Phi) = 0, \\ \Phi(0,\cdot) = \Phi_0, \qquad \Phi(T,\cdot) = \Phi_T. \end{cases} \tag{1}$$

$A(u,v) = (-v, -\Delta u + \alpha u)$, $\mathbf{F} = (0, f)$, $G(\Phi) = (0, g(u))$.
$\Phi_0 = (u^0, u^1)$, $\Phi_T = (u_T^0, u_T^1)$.
1D example: $\Omega = (0,1)$, $\alpha = 0$, $T = 2.5$, $g(u) = \beta \tanh u$; target: rest.

Why $H_0^1(\Omega) \times L^2(\Omega)$?

The wave state $\Phi = (u, v)$, with $v = u_t$, records both deformation and motion.

Displacement: deformation energy

$$E_{\text{def}} = \tfrac{1}{2} \int_\Omega |\nabla u|^2 \, \mathrm{d}x$$

Finite energy + zero boundary values

$$u \in H_0^1(\Omega)$$

Velocity: kinetic energy

$$E_{\text{kin}} = \tfrac{1}{2} \int_\Omega |v|^2 \, \mathrm{d}x$$

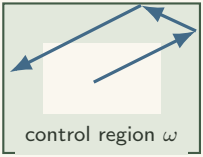
Finite energy $\rightarrow$ square-integrable velocity

$$v = u_t \in L^2(\Omega)$$

$$\Phi = (u, u_t) \in \mathcal{E} = H_0^1(\Omega) \times L^2(\Omega)$$

Finite energy + fixed boundary values give the natural state space.

Geometry, Observability, and Controllability

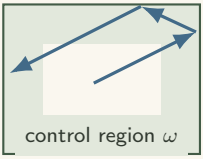


ray picture

Geometric Control Condition (GCC)

Every relevant geometric-optics ray must enter ω before time T.

Geometry, Observability, and Controllability



ray picture

Geometric Control Condition (GCC)

Every relevant geometric-optics ray must enter ω before time T.

HUM duality theorem: the linear wave ($g = 0$)

Exact controllability: every $\Phi_0, \Phi_T \in \mathcal{E}$ can be connected in time T by some $f \in L^2((0,T) \times \omega)$

if and only if the following **observability estimate** holds for every homogeneous adjoint wave p, with one constant $C_{\text{obs}} > 0$:

$$\|(p(0), p_t(0))\|_{\mathcal{E}}^2 \leq C_{\text{obs}} \int_0^T \|p_t(t)\|_{L^2(\omega)}^2 \, \mathrm{d}t, \qquad p_{tt} - \Delta p + \alpha p = 0, \quad p|_{\partial\Omega} = 0.$$

[Lions, 1988, Bardos et al., 1992].

Foundations of Wave Controllability

- **HUM** [Lions, 1988]
  Observe the adjoint wave; solve a minimum-norm control problem.
- **Geometric observability** [Bardos et al., 1992]
  Track rays to identify when observation and control are possible.
- **Semilinear waves** [Zuazua, 1993, Dehman and Lebeau, 2009]
  Use linear control mechanisms to handle nonlinear state transfers.
- **Control and numerics** [Ervedoza and Zuazua, 2012]
  A convergent forward scheme need not preserve control properties.

Foundations of Wave Controllability

- **HUM** [Lions, 1988]
  Observe the adjoint wave; solve a minimum-norm control problem.
- **Geometric observability** [Bardos et al., 1992]
  Track rays to identify when observation and control are possible.
- **Semilinear waves** [Zuazua, 1993, Dehman and Lebeau, 2009]
  Use linear control mechanisms to handle nonlinear state transfers.
- **Control and numerics** [Ervedoza and Zuazua, 2012]
  A convergent forward scheme need not preserve control properties.

We build on this control theory; we do not replace it.

Constructive and Learning-Based Approaches

Deterministic reconstruction

[Münch and Trélat, 2022]
Least-squares construction for semilinear 1D waves.

[Claret et al., 2024]
Fixed-point methods for semilinear boundary controllability.

Learned reconstruction

[Mowlavi and Nabi, 2023]
Physics-informed neural PDE control.

[Du et al., 2024, Feng et al., 2025]
Learn in spectral coordinates; use spatial structure.

Constructive and Learning-Based Approaches

Deterministic reconstruction

[Münch and Trélat, 2022]
Least-squares construction for semilinear 1D waves.

[Claret et al., 2024]
Fixed-point methods for semilinear boundary controllability.

Learned reconstruction

[Mowlavi and Nabi, 2023]
Physics-informed neural PDE control.

[Du et al., 2024, Feng et al., 2025]
Learn in spectral coordinates; use spatial structure.

Our focus: prove that the computed control works, rather than rely only on a small training loss.

Our Main Contributions

1. Compute a control

We use learned and classical methods to find a force aimed at the desired final state.

2. Improve its accuracy

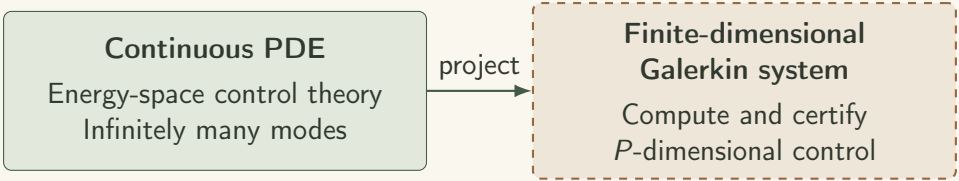
We correct the computed force to reduce the error in the wave's final shape and velocity.

3. Prove an exact control is nearby

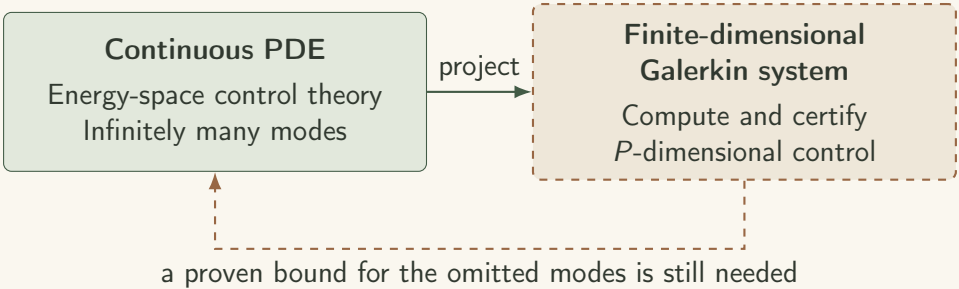
We bound the numerical errors and, when the checks pass, prove that an exact control exists within a known distance of the computed one, for the finite model.

Compute a control, correct it, and prove an exact control is nearby.

The PDE and Its Finite-Dimensional Model



The PDE and Its Finite-Dimensional Model



Exact control of the P-mode model does not imply exact control of the full PDE.

Spectral Galerkin Discretization

On $\Omega = (0,1)^N$, the Dirichlet eigenfunctions and eigenvalues are

$$e_k(x) = 2^{N/2} \prod_{\ell=1}^{N} \sin(k_\ell \pi x_\ell), \qquad \mu_k = \pi^2 \sum_{\ell=1}^{N} k_\ell^2, \qquad k \in \{1, 2, \dots\}^N.$$

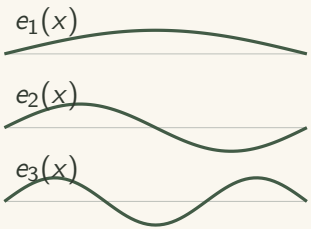


Illustration: first three 1D modes.

A finite retained set is relabeled as $e_1, \dots, e_P$, with corresponding eigenvalues $\mu_1, \dots, \mu_P$.

$$u_P(t,x) = \sum_{j=1}^{P} a_j(t) e_j(x).$$

Spectral Galerkin Discretization

On $\Omega = (0,1)^N$, the Dirichlet eigenfunctions and eigenvalues are

$$e_k(x) = 2^{N/2} \prod_{\ell=1}^{N} \sin(k_\ell \pi x_\ell), \qquad \mu_k = \pi^2 \sum_{\ell=1}^{N} k_\ell^2, \qquad k \in \{1, 2, \dots\}^N.$$

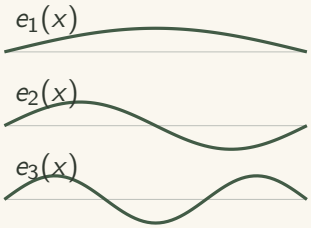


Illustration: first three 1D modes.

A finite retained set is relabeled as $e_1, \dots, e_P$, with corresponding eigenvalues $\mu_1, \dots, \mu_P$.

$$u_P(t,x) = \sum_{j=1}^{P} a_j(t) e_j(x).$$

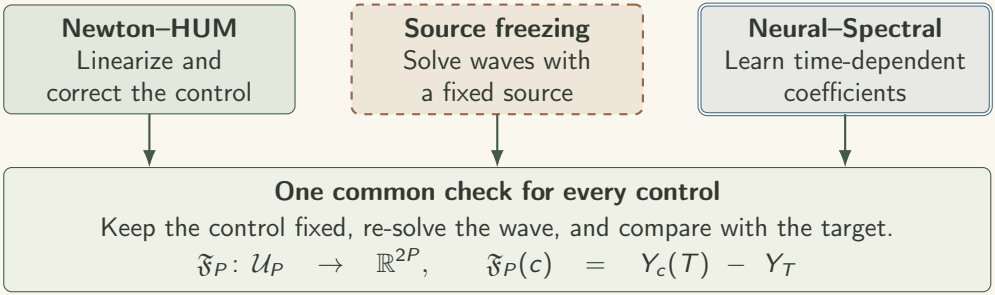
$$\boxed{a'' + \Lambda_P a + G_P(a) + M_P c = 0}$$

$$\Lambda_P = \mathrm{diag}(\mu_1, \dots, \mu_P), \qquad (M_P)_{j\ell} = \int_\omega e_j e_\ell \, \mathrm{d}x.$$

$G_P(a)$ is the nonlinearity projected onto these modes.

The basis enforces $u_P = 0$ on $\partial\Omega$. We solve for the time-dependent state coefficients $a_j(t)$ and control coefficients $c_j(t)$.

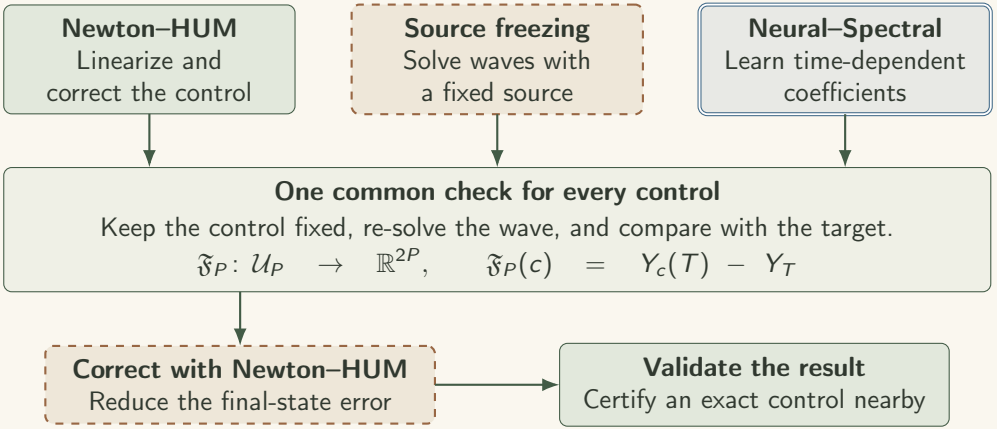
A Common Endpoint Formulation



$\mathcal{U}_P := L^2\Big(0, T; \mathbb{R}^P\Big)$; $Y = \Big(\Lambda_P^{1/2} a,\, a'\Big)$ uses energy coordinates.

Control norms are in $\mathcal{U}_P$, endpoint norms are Euclidean, and operator norms are induced by these norms.

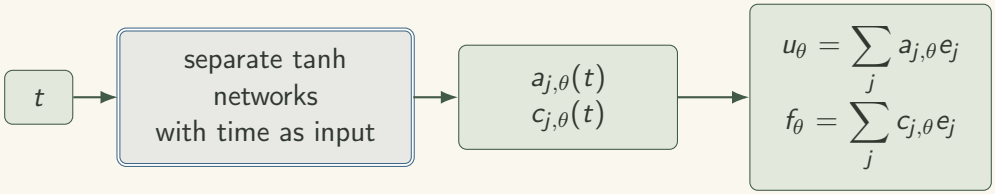
A Common Endpoint Formulation



$\mathcal{U}_P := L^2\Big(0, T; \mathbb{R}^P\Big)$; $Y = \Big(\Lambda_P^{1/2} a,\, a'\Big)$ uses energy coordinates.

Control norms are in $\mathcal{U}_P$, endpoint norms are Euclidean, and operator norms are induced by these norms.

Neural–Spectral Control Reconstruction



$$a_{j,\theta}(t) = \sum_{m=1}^{W} v_{jm}^{a} \tanh\left(w_{jm}^{a} t + b_{jm}^{a}\right),$$

and similarly for $c_{j,\theta}$; derivatives come from automatic differentiation.

Spatial properties and boundary conditions are built in eigenfunctions.

Does the learned state follow the wave dynamics?

$r_\theta = a_\theta'' + \Lambda_P a_\theta + G_P(a_\theta) + M_P c_\theta$.

Training loss:

$$\mathcal{J}(\theta) = \frac{T}{N_c+1} \sum_{q=1}^{N_c} \|r_\theta(t_q)\|_2^2 + 500\Big(\|Y_\theta(0) - Y_0\|_2^2 + \|Y_\theta(T) - Y_T\|_2^2\Big).$$

Here $t_q = qT/(N_c+1)$ are the N_c interior sample times and $Y_\theta = (\Lambda_P^{1/2} a_\theta, a_\theta')$. Y_0, Y_T are the prescribed initial and target states in energy coordinates.

Does the learned state follow the wave dynamics?

$r_\theta = a_\theta'' + \Lambda_P a_\theta + G_P(a_\theta) + M_P c_\theta$.

Training loss:

$$\mathcal{J}(\theta) = \frac{T}{N_c+1} \sum_{q=1}^{N_c} \|r_\theta(t_q)\|_2^2 + 500\Big(\|Y_\theta(0) - Y_0\|_2^2 + \|Y_\theta(T) - Y_T\|_2^2\Big).$$

Here $t_q = qT/(N_c+1)$ are the N_c interior sample times and $Y_\theta = (\Lambda_P^{1/2} a_\theta, a_\theta')$. Y_0, Y_T are the prescribed initial and target states in energy coordinates.

What the analysis does guarantee

Assume the P-mode solution driven by c_θ, starting from the prescribed initial data, exists throughout $[0, T]$, and $\|DG_P\| \le \ell_1$ along the connecting segments. Put $\kappa = \ell_1/(2\pi)$.

$$\sup_{0\le t\le T} \left\|\Phi_\theta^P(t) - \Phi_{c_\theta}^P(t)\right\|_{\mathcal{E}} \le e^{\kappa T}\left(e_{\text{initial}} + \|r_\theta\|_{L^1(0,T;\mathbb{R}^P)}\right).$$

Here $e_{\text{initial}} = \|Y_\theta(0) - Y_0\|_2$ and Φ_{c_θ} is the independently solved P-mode state.

Does the learned control bring the system close to the target?

Compare the independently solved P-mode state with the target:

$E_{\mathrm{tar}}(P)$
projection
error

E_{net}
network
approximation
error

η_Q
integration
error

E_{opt}
optimization
error

Does the learned control bring the system close to the target?

Compare the independently solved P-mode state with the target:

$E_{\mathrm{tar}}(P)$ projection error

E_{net} network approximation error

η_Q integration error

E_{opt} optimization error

$$\left\| \Phi^P_{c_\theta}(T) - \Phi_T \right\|_{\mathcal{E}} \leq E_{\mathrm{tar}}(P) + C\big(E_{\mathrm{net}} + \eta_Q + E_{\mathrm{opt}}\big).$$

Assumptions. The P-mode solution driven by c_θ exists throughout $[0, T]$ from the prescribed initial data, with the derivative bound above; fixed positive quadrature and endpoint weights; a uniform quadrature bound on a bounded parameter set containing θ.

Linearized Controllability and the HUM Right Inverse

Question: Which control change cancels the current endpoint error $r = \mathfrak{F}_P(c)$?

◇ **Predict the endpoint change.** Set $C_c = D\mathfrak{F}_P(c)$.

$$\mathfrak{F}_P(c + \delta c) \approx r + C_c \delta c.$$

We therefore seek $C_c \delta c = -r$.

Linearized Controllability and the HUM Right Inverse

Question: Which control change cancels the current endpoint error $r = \mathfrak{F}_P(c)$?

◇ **Predict the endpoint change.** Set $C_c = D\mathfrak{F}_P(c)$.

$$\mathfrak{F}_P(c + \delta c) \approx r + C_c \delta c.$$

We therefore seek $C_c \delta c = -r$.

◇ **Find a minimum-norm correction.** For $W_c = C_c C_c^* > 0$, define the **right inverse**

$$R_c = C_c^* W_c^{-1}, \qquad C_c R_c = I.$$

Choose $\delta c = -R_c r$, the minimum-norm solution:
$C_c \delta c = -C_c R_c r = -r$.
We use $C_c R_c = I$, not $R_c C_c = I$.

Linearized Controllability and the HUM Right Inverse

Question: Which control change cancels the current endpoint error $r = \mathfrak{F}_P(c)$?

◇ **Predict the endpoint change.** Set $C_c = D\mathfrak{F}_P(c)$.

$$\mathfrak{F}_P(c + \delta c) \approx r + C_c \delta c.$$

We therefore seek $C_c \delta c = -r$.

◇ **Find a minimum-norm correction.** For $W_c = C_c C_c^* > 0$, define the **right inverse**

$$R_c = C_c^* W_c^{-1}, \qquad C_c R_c = I.$$

Choose $\delta c = -R_c r$, the minimum-norm solution:
$C_c \delta c = -C_c R_c r = -r$.
We use $C_c R_c = I$, not $R_c C_c = I$.

◇ **Measure the effort:** $\|R_c\| = \lambda_{\min}(W_c)^{-1/2}$.
Small eigenvalues mean costly correction directions.

Why solve again?

Predicted error: $r + C_c \delta c = 0$.

Actual error: the nonlinear remainder remains:

$$\mathfrak{F}_P(c + \delta c) = \mathcal{R}_c(\delta c).$$

Here $\mathcal{R}_c$ is the part omitted by the linear approximation; it need not be zero.

Check: Re-solve the nonlinear P-mode system with $c + \delta c$ and the same initial data. Measure its error at T.

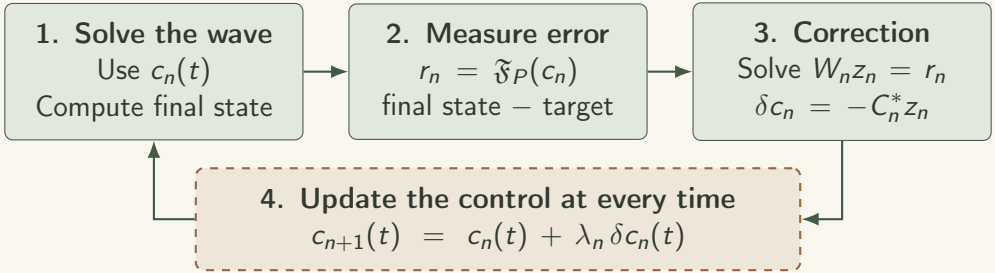
Cancel the predicted error, then re-solve to measure the actual error.

HUM = Hilbert Uniqueness Method. Background: [Lions, 1988, Dehman and Lebeau, 2009].

Newton–HUM Endpoint Correction

Here $c_n(t) \in \mathbb{R}^P$ is the current control: one time-dependent coefficient per mode.

$$C_n = D\mathfrak{F}_P(c_n), \qquad W_n = C_n C_n^*.$$

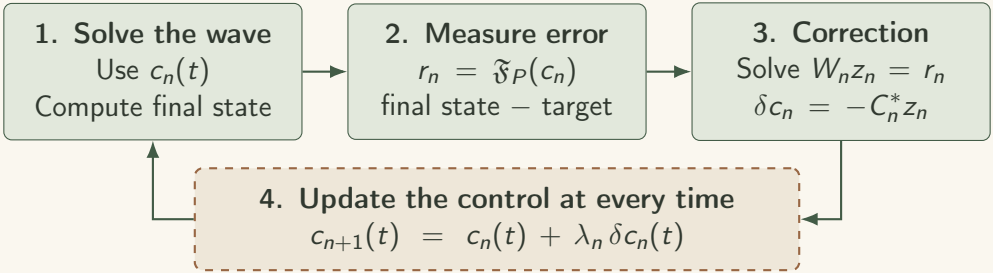


Choose the step: try $\lambda_n = 1, 1/2, 1/4, \ldots$; keep the first step that reduces the final-state error. Repeat until the tolerance is met.

Newton–HUM Endpoint Correction

Here $c_n(t) \in \mathbb{R}^P$ is the current control: one time-dependent coefficient per mode.

$$C_n = D\mathfrak{F}_P(c_n), \qquad W_n = C_n C_n^*.$$



Choose the step: try $\lambda_n = 1, 1/2, 1/4, \ldots$; keep the first step that reduces the final-state error. Repeat until the tolerance is met.

This method reduces the error quadratically.

An Error Certificate for Any Solver

Endpoint error
$\|\mathfrak{F}_P(\bar{c})\| \leq \varepsilon$
How far did we miss?

Controllability
$\|R_{\bar{c}}\| \leq \gamma$
How hard is it to correct this error?

Nonlinearity
$\mathrm{Lip}(D\mathfrak{F}_P) \leq L$
How curved is the endpoint map?

An Error Certificate for Any Solver

Endpoint error
$\|\mathfrak{F}_P(\bar{c})\| \le \varepsilon$
How far did we miss?

Controllability
$\|R_{\bar{c}}\| \le \gamma$
How hard is it to correct this error?

Nonlinearity
$\mathrm{Lip}(D\mathfrak{F}_P) \le L$
How curved is the endpoint map?

A rigorous check after computing the control

Back to overview

Suppose $\mathfrak{F}_P$ is C^1, $D\mathfrak{F}_P(\bar{c})R_{\bar{c}} = I$, and $L > 0$. If

$$h = 2L\gamma^2\varepsilon < 1, \qquad d_* := \frac{1 - \sqrt{1-h}}{L\gamma}$$

and the radius-d_* ball stays in the neighborhood where L applies, then there is a control c^* for the P-mode system with $\mathfrak{F}_P(c^*) = 0$ and $\|c^* - \bar{c}\|_{L^2(0,T;\mathbb{R}^P)} \le d_*$.

Proof Strategy: Reduce to a Fixed-Point Equation

Write $R = R_{\bar{c}}$, with $D\mathfrak{F}_P(\bar{c})R = I$, $\|R\| \le \gamma$ and $\|\mathfrak{F}_P(\bar{c})\| \le \varepsilon$. Assume $D\mathfrak{F}_P$ is L-Lipschitz on a neighborhood containing the certified control ball.

◇ **Use endpoint coordinates for corrections.**
Seek $c = \bar{c} + Ry$, where $y \in \mathbb{R}^{2P}$ and $Ry \in L^2(0, T; \mathbb{R}^P)$. Define

$$H(y) = \mathfrak{F}_P(\bar{c} + Ry).$$

By the chain rule and $D\mathfrak{F}_P(\bar{c})R = I$,

$$DH(0) = D\mathfrak{F}_P(\bar{c})R = I.$$

Proof Strategy: Reduce to a Fixed-Point Equation

Write $R = R_{\bar{c}}$, with $D\mathfrak{F}_P(\bar{c})R = I$, $\|R\| \le \gamma$ and $\|\mathfrak{F}_P(\bar{c})\| \le \varepsilon$. Assume $D\mathfrak{F}_P$ is L-Lipschitz on a neighborhood containing the certified control ball.

◇ **Use endpoint coordinates for corrections.**
Seek $c = \bar{c} + Ry$, where $y \in \mathbb{R}^{2P}$ and $Ry \in L^2(0, T; \mathbb{R}^P)$. Define

$$H(y) = \mathfrak{F}_P(\bar{c} + Ry).$$

By the chain rule and $D\mathfrak{F}_P(\bar{c})R = I$,

$$DH(0) = D\mathfrak{F}_P(\bar{c})R = I.$$

◇ **Separate the nonlinear remainder.**

$$Q(y) := H(y) - H(0) - y, \qquad Q(0) = 0.$$

Thus the desired endpoint equation becomes

$$H(y) = 0 \iff y = \underbrace{-H(0) - Q(y)}_{\mathcal{T}(y)}.$$

◇ **Bound the nonlinear remainder.**

$$DQ(y) = [D\mathfrak{F}_P(\bar{c} + Ry) - D\mathfrak{F}_P(\bar{c})]R,$$

$$\|DQ(y)\| \le L\,\|Ry\|\,\|R\| \le L\gamma^2\,\|y\|.$$

Integrating along the segment from 0 to y,

$$Q(y) = \int_0^1 DQ(sy)y\,\mathrm{d}s,$$

$$\|Q(y)\| \le \int_0^1 L\gamma^2 s\,\|y\|^2\,\mathrm{d}s = \tfrac{1}{2}L\gamma^2\,\|y\|^2.$$

For $\|y\|, \|z\| \le r$, their connecting segment also lies in the ball, so

$$\|Q(y) - Q(z)\| \le L\gamma^2 r\,\|y - z\|.$$

Proof Strategy: Close the Ball and Obtain an Exact Control

Recall $\mathcal{T}(y) = -H(0) - Q(y)$ and $H(y) = \mathfrak{F}_P(\bar{c} + Ry)$. Set $h = 2L\gamma^2\varepsilon < 1$, with $L > 0$.

◇ **Choose a ball that maps into itself.** For $\|y\| \le r$, the remainder bound gives

$$\|\mathcal{T}(y)\| \le \varepsilon + \tfrac{1}{2}L\gamma^2 r^2.$$

Choose the smaller root of $\varepsilon + \frac{1}{2}L\gamma^2 r^2 = r$:

$$r_* := \frac{1 - \sqrt{1-h}}{L\gamma^2}.$$

Then $\mathcal{T}$ maps $\overline{B}_{r_*}(0)$ into itself.

Check the domain: $\|Ry\| \le \gamma r_* = d_*$. The theorem assumes the closed control ball of radius d_* lies in the neighborhood where the derivative bound holds.

Proof Strategy: Close the Ball and Obtain an Exact Control

Recall $\mathcal{T}(y) = -H(0) - Q(y)$ and $H(y) = \mathfrak{F}_P(\bar{c} + Ry)$. Set $h = 2L\gamma^2\varepsilon < 1$, with $L > 0$.

◇ **Choose a ball that maps into itself.** For $\|y\| \le r$, the remainder bound gives

$$\|\mathcal{T}(y)\| \le \varepsilon + \tfrac{1}{2}L\gamma^2 r^2.$$

Choose the smaller root of $\varepsilon + \frac{1}{2}L\gamma^2 r^2 = r$:

$$r_* := \frac{1 - \sqrt{1-h}}{L\gamma^2}.$$

Then $\mathcal{T}$ maps $\overline{B}_{r_*}(0)$ into itself.

Check the domain: $\|Ry\| \le \gamma r_* = d_*$. The theorem assumes the closed control ball of radius d_* lies in the neighborhood where the derivative bound holds.

◇ **Show strict contraction.** For $y, z \in \overline{B}_{r_*}(0)$,

$$\|\mathcal{T}(y) - \mathcal{T}(z)\| \le L\gamma^2 r_* \|y - z\|,$$

and $L\gamma^2 r_* = 1 - \sqrt{1-h} < 1$.

◇ **Apply Banach's fixed-point theorem.** The closed ball in $\mathbb{R}^{2P}$ is complete. Hence it contains a unique fixed point y^*, giving

$$c^* = \bar{c} + Ry^*, \qquad \mathfrak{F}_P(c^*) = 0,$$

$$\|c^* - \bar{c}\|_{L^2} \le \gamma r_* = \frac{1 - \sqrt{1-h}}{L\gamma} = d_*.$$

Uniqueness holds only in the slice $\bar{c} + R\overline{B}_{r_*}(0)$: R is injective because $D\mathfrak{F}_P(\bar{c})R = I$.

Source-Frozen HUM: What We Solve at Each Step

Idea: freeze the nonlinear source, then solve a linear steering problem.

◇ **Freeze the source.** Start with a trajectory guess $a^{(n)}(t)$ and compute

$$s_n(t) = G_P(a^{(n)}(t)).$$

Keep this entire time-dependent function fixed during the next solve.

◇ **Solve for a new trajectory and control.**

$$(a^{(n+1)})'' + \Lambda_P a^{(n+1)}$$
$$+ s_n + M_P c^{(n+1)} = 0.$$

Use the prescribed initial and final displacement and velocity. The unknowns are $a^{(n+1)}$ and $c^{(n+1)}$.

Source-Frozen HUM: What We Solve at Each Step

Idea: freeze the nonlinear source, then solve a linear steering problem.

◇ **Freeze the source.** Start with a trajectory guess $a^{(n)}(t)$ and compute

$$s_n(t) = G_P(a^{(n)}(t)).$$

Keep this entire time-dependent function fixed during the next solve.

◇ **Solve for a new trajectory and control.**

$$(a^{(n+1)})'' + \Lambda_P a^{(n+1)} + s_n + M_P c^{(n+1)} = 0.$$

Use the prescribed initial and final displacement and velocity. The unknowns are $a^{(n+1)}$ and $c^{(n+1)}$.

◇ **Which steering control do we choose?** Among controls that reach those endpoints, HUM selects the one minimizing the coefficient cost

$$\int_0^T \|c(t)\|^2 \, \mathrm{d}t.$$

The next slide shows how a matrix called the **Gramian** computes this control.

◇ **Update the source and repeat.** Set $s_{n+1} = G_P(a^{(n+1)})$ and solve again. At a fixed point a^*, the source used in the solve is exactly $G_P(a^*)$.

Freeze a source, find its minimum-cost steering control, then update the source.

The Gramian: From an Endpoint Gap to a Control

Let $Y = (\Lambda_P^{1/2} a, a') \in \mathbb{R}^{2P}$ collect displacement and velocity. Fix P, T, the wave operator, and the control region.

◇ **Find the endpoint gap.** Solve the frozen-source wave with $c = 0$ to obtain $Y_n^{\mathrm{free}}(T)$. The control must supply

$$d_n = Y_T - Y_n^{\mathrm{free}}(T).$$

Let $K(t) \in \mathbb{R}^{2P \times P}$ map a control input at time t to its effect at T. Then

$$Y(T) = Y_n^{\mathrm{free}}(T) + \int_0^T K(t) c(t)\, \mathrm{d}t.$$

◇ **Collect the control effects in one matrix.**

$$\boxed{W_T = \int_0^T K(t) K(t)^\top \, \mathrm{d}t}$$

This $2P \times 2P$ matrix is the **controllability Gramian**. It measures how strongly controls can change each endpoint direction.

The Gramian: From an Endpoint Gap to a Control

Let $Y = (\Lambda_P^{1/2} a, a') \in \mathbb{R}^{2P}$ collect displacement and velocity. Fix P, T, the wave operator, and the control region.

◇ **Find the endpoint gap.** Solve the frozen-source wave with $c = 0$ to obtain $Y_n^{\mathrm{free}}(T)$. The control must supply

$$d_n = Y_T - Y_n^{\mathrm{free}}(T).$$

Let $K(t) \in \mathbb{R}^{2P \times P}$ map a control input at time t to its effect at T. Then

$$Y(T) = Y_n^{\mathrm{free}}(T) + \int_0^T K(t) c(t)\,\mathrm{d}t.$$

◇ **Collect the control effects in one matrix.**

$$\boxed{W_T = \int_0^T K(t) K(t)^\top \,\mathrm{d}t}$$

This $2P \times 2P$ matrix is the **controllability Gramian**. It measures how strongly controls can change each endpoint direction.

◇ **Compute the HUM control.** For a positive-definite W_T, solve and reconstruct:

$$W_T z_n = d_n, \qquad c^{(n+1)}(t) = K(t)^\top z_n.$$

It supplies exactly the missing endpoint change:

$$\int_0^T K(t) c^{(n+1)}(t)\,\mathrm{d}t = W_T z_n = d_n.$$

This is exactly the **minimum-coefficient-cost control selected by HUM**.

The next slide derives $K(t)$ and explains why the same Gramian works at every source-frozen iteration.

Why Can We Reuse the Gramian?

Keep fixed: P, T, the wave operator, the control region, and the coefficient cost.

◇ **Separate the wave from the source.** For $Y = (\Lambda_P^{1/2} a, a')$, the frozen equation is

$$Y' = AY + Bc + f_n(t), \qquad f_n = \begin{pmatrix} 0 \\ -s_n \end{pmatrix}.$$

$$A = \begin{pmatrix} 0 & \Lambda_P^{1/2} \\ -\Lambda_P^{1/2} & 0 \end{pmatrix}, \qquad B = \begin{pmatrix} 0 \\ -M_P \end{pmatrix}.$$

Only f_n changes; A and B stay fixed.

◇ **What does $K(t)$ do?**

$$\boxed{K(t) = e^{A(T-t)} B}$$

B applies the control; $e^{A(T-t)}$ carries its effect to T. $K(t)$ varies with **time**, but stays the same across **iterations**.

Why Can We Reuse the Gramian?

Keep fixed: P, T, the wave operator, the control region, and the coefficient cost.

◇ **Separate the wave from the source.** For $Y = (\Lambda_P^{1/2} a, a')$, the frozen equation is

$$Y' = AY + Bc + f_n(t), \qquad f_n = \begin{pmatrix} 0 \\ -s_n \end{pmatrix}.$$

$$A = \begin{pmatrix} 0 & \Lambda_P^{1/2} \\ -\Lambda_P^{1/2} & 0 \end{pmatrix}, \qquad B = \begin{pmatrix} 0 \\ -M_P \end{pmatrix}.$$

Only f_n changes; A and B stay fixed.

◇ **What does $K(t)$ do?**

$$\boxed{K(t) = e^{A(T-t)}B}$$

B applies the control; $e^{A(T-t)}$ carries its effect to T. $K(t)$ varies with **time**, but stays the same across **iterations**.

◇ **What changes at the endpoint?** With zero control, the frozen source gives

$$Y_n^{\mathrm{free}}(T) = e^{AT} Y(0) + \int_0^T e^{A(T-t)} f_n(t)\,\mathrm{d}t.$$

Adding a control gives

$$Y(T) = Y_n^{\mathrm{free}}(T) + \int_0^T K(t)c(t)\,\mathrm{d}t.$$

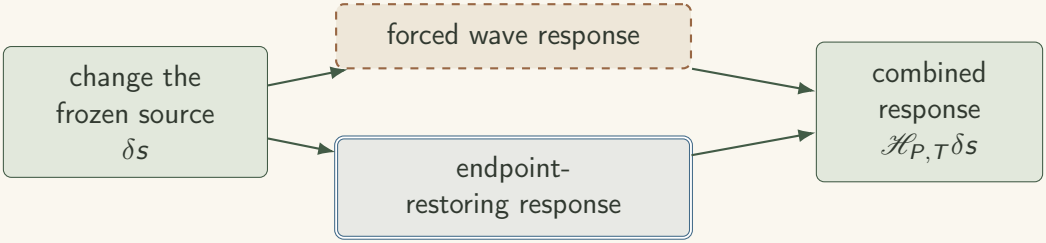
So the gap $d_n = Y_T - Y_n^{\mathrm{free}}(T)$ changes, while

$$W_T = \int_0^T K(t)K(t)^\top\,\mathrm{d}t$$

stays fixed.

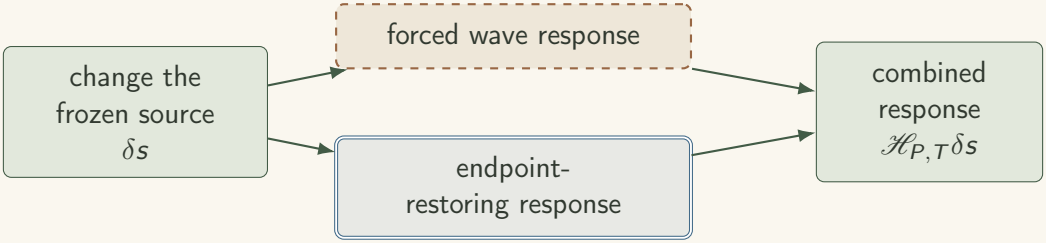
◇ **Compute once, reuse many times.** Factor the positive-definite W_T once. Reuse its factors to solve $W_T z_n = d_n$ for each new gap, then set $c^{(n+1)}(t) = K(t)^\top z_n$.

Bounding the Combined Response



Combine the responses to retain cancellation: $\chi_{P,T}$ is the largest displacement gain; ℓ_g is the scalar Lipschitz constant of g.

Bounding the Combined Response



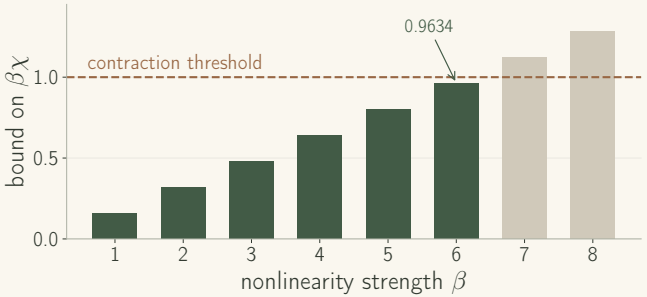
Combine the responses to retain cancellation: $\chi_{P,T}$ is the largest displacement gain; ℓ_g is the scalar Lipschitz constant of g.

$$\chi_{P,T} := \|\mathscr{H}_{P,T}\|_{\mathcal{L}\left(L^2\left(0,T;\mathbb{R}^P\right)\right)},$$

$$\|\mathcal{T}_P(a) - \mathcal{T}_P(b)\|_{L^2\left(0,T;\mathbb{R}^P\right)} \le \ell_g \chi_{P,T} \|a - b\|_{L^2\left(0,T;\mathbb{R}^P\right)}.$$

If $q = \ell_g \chi_{P,T} < 1$, each update shrinks trajectory differences by at most q; source freezing converges.

A Contraction Bound for the P-Mode System



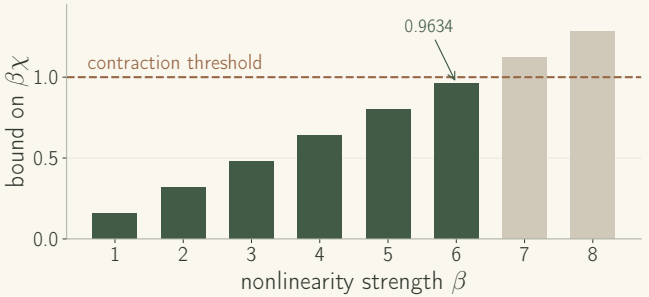
$P = 8$, $T = 2.5$, collar width 0.3; coefficient cost.

Each bar is β times the proven upper bound for $\chi_{P,T}$. A bar below 1 certifies contraction.

Proven bound:

$$\chi_{8,2.5} < 0.160561.$$

A Contraction Bound for the P-Mode System



$P = 8$, $T = 2.5$, collar width 0.3; coefficient cost.

Each bar is β times the proven upper bound for $\chi_{P,T}$. A bar below 1 certifies contraction.

Proven bound:

$$\chi_{8,2.5} < 0.160561.$$

For $g(u) = \beta \tanh u$, $\ell_g = \beta$: **Global contraction for** $0 \le \beta \le 6$.

For this 8-mode model and $0 \le \beta \le 6$, source freezing converges from any initial trajectory guess.

Numerical Results: What We Prove and Observe

Theorems certify retained controls; experiments compare accuracy, effort, and cost.

Proved: convergence

For the 8-mode tanh model at $T = 2.5$, source freezing converges from any starting guess when $0 \le \beta \le 6$.

Proved: nearby exact controls

At $P = 8$, $\beta = 1$, exact controls lie near all three tested controls.

Finer checks ($500 \to 4000$ time cells) give tighter distance bounds.

Observed in our experiments

- **Accurate tanh controls.** Both classical methods reach error $< 10^{-8}$ at $P = 8, 12, 16$.
- **Learned controls:** all six reach 10^{-8} in exactly two accepted Newton–HUM steps.
- **More modes:** $P = 8 \to 32$ cuts error $8.51\times$ in a fixed 128-mode check.
- **2D:** spectral networks improve on PINNs; Gramian controls give lower error and effort.
- **Cubic** $-11u^3$**:** gradual parameter changes + Newton–HUM work at $P = 8, 12, 16$.

Numerical Setup and Accuracy Checks

$T = 2.5$, $\omega = (0, 0.3) \cup (0.7, 1)$, target: zero displacement and velocity; $P = 8, 12, 16$.

$$a(0) = \tfrac{1}{\sqrt{2}}\,(1,\ 0.5,\ -0.3,\ 0, \ldots)\,, \qquad a'(0) = 0.$$

E_K: terminal energy-norm distance from rest in an independent nonlinear K-mode solve.

Model check

Does it reach the target?

Use the computed control in a separate nonlinear P-mode forward solve.

Require $E_P \leq 10^{-8}$: terminal displacement and velocity are close to zero in this model.

More modes

Does it work at finer resolution?

Keep the control fixed. Solve with $K = 2P$, $4P$, or 128, as specified in each test.

Report E_K to assess omitted modes. Smaller means closer to the target in the richer model.

Effort and time

What does steering cost?

Effort: $\|\mathbf{1}_\omega f_P\|_{L^2}$ measures applied input size over space and time.

Runtime: includes continuation, backtracking, and correction. Neural training is reported separately.

Numerical Setup and Accuracy Checks

$T = 2.5$, $\omega = (0, 0.3) \cup (0.7, 1)$, target: zero displacement and velocity; $P = 8, 12, 16$.

$$a(0) = \tfrac{1}{\sqrt{2}}\,(1,\ 0.5,\ -0.3,\ 0, \ldots), \qquad a'(0) = 0.$$

E_K: terminal energy-norm distance from rest in an independent nonlinear K-mode solve.

Model check

Does it reach the target?

Use the computed control in a separate nonlinear P-mode forward solve.

Require $E_P \leq 10^{-8}$: terminal displacement and velocity are close to zero in this model.

More modes

Does it work at finer resolution?

Keep the control fixed. Solve with $K = 2P$, $4P$, or 128, as specified in each test.

Report E_K to assess omitted modes. Smaller means closer to the target in the richer model.

Effort and time

What does steering cost?

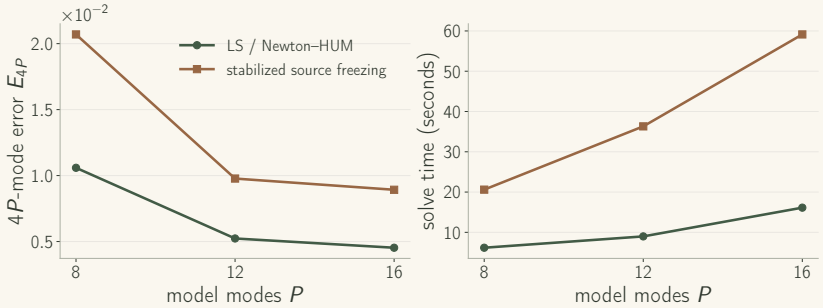
Effort: $\|\mathbf{1}_\omega f_P\|_{L^2}$ measures applied input size over space and time.

Runtime: includes continuation, backtracking, and correction. Neural training is reported separately.

Timing: one CPU thread; excludes one-time assembly and independent accuracy checks.

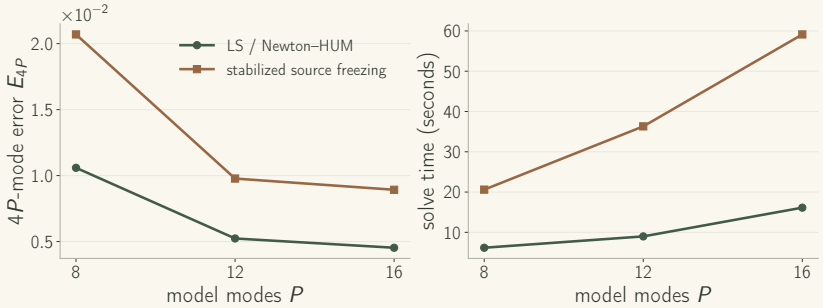
Matched Comparison of Deterministic Methods

Matched $g(u) = 6 \tanh u$ runs; every control has $E_P < 10^{-8}$. Compare runtime, higher-resolution error, and applied effort at each P.



Matched Comparison of Deterministic Methods

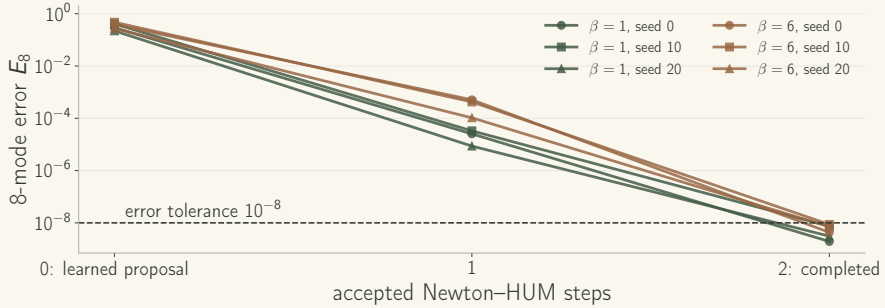
Matched $g(u) = 6 \tanh u$ runs; every control has $E_P < 10^{-8}$. Compare runtime, higher-resolution error, and applied effort at each P.



For these matched $\beta = 6$ tests, Newton–HUM gives lower runtime, higher-resolution error, and control effort.

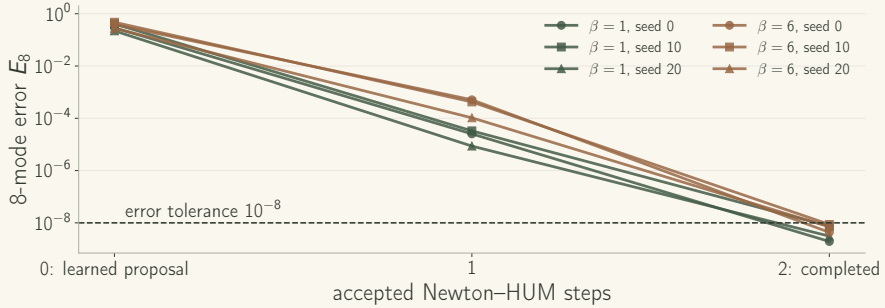
Newton–HUM Correction of Learned Controls

Use the trained control as a starting guess, then cancel its endpoint residual with Newton–HUM updates.



Newton–HUM Correction of Learned Controls

Use the trained control as a starting guess, then cancel its endpoint residual with Newton–HUM updates.



All six learned candidates go from errors 0.222–0.473 to $< 10^{-8}$ in two accepted corrections.

Computational Cost and Control Effort

Correction time is additional to training. The physical norm measures the applied control after correction.

$P = 8$, $\beta \in \{1, 6\}$	Time (s)	Physical norm
Direct Newton–HUM	3.53–6.18	5.14–6.30
Newton–HUM correction	2.6–3.2	10.6–16.8

Computational Cost and Control Effort

Correction time is additional to training. The physical norm measures the applied control after correction.

$P = 8$, $\beta \in \{1, 6\}$	Time (s)	Physical norm
Direct Newton–HUM	3.53–6.18	5.14–6.30
Newton–HUM correction	2.6–3.2	10.6–16.8

Completing these six learned candidates

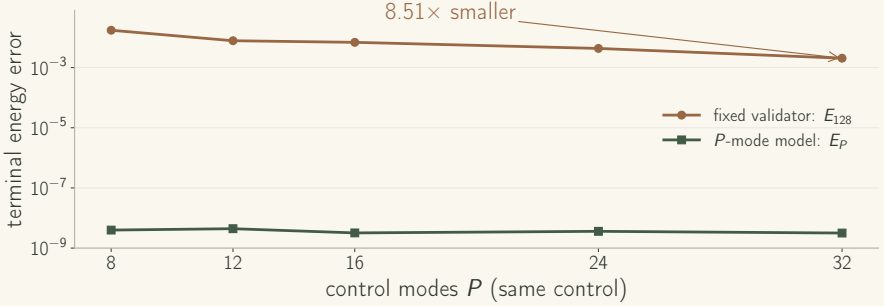
Correction adds 2.6–3.2 seconds to reach the model tolerance. The completed controls can then be assessed using the certificate inputs.

For these single-problem benchmarks

Direct Newton–HUM is the lower-cost route in both runtime and physical control effort.

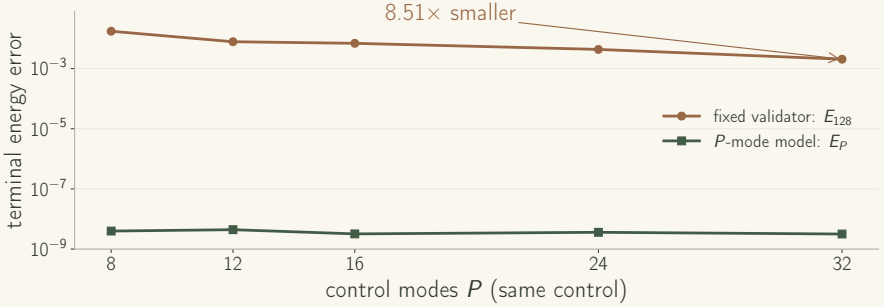
Omitted Modes and a Fixed Accuracy Check

$g(u) = \tanh u$. Increase the reconstruction size P, but evaluate every resulting control in the same 128-mode system.



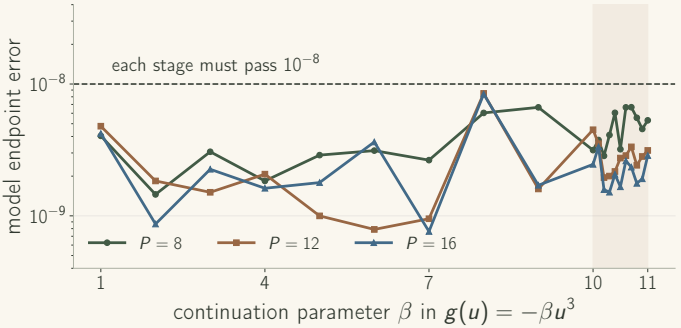
Omitted Modes and a Fixed Accuracy Check

$g(u) = \tanh u$. Increase the reconstruction size P, but evaluate every resulting control in the same 128-mode system.



Increasing P from 8 to 32 reduces the fixed-validator endpoint error by 8.51× in this experiment.

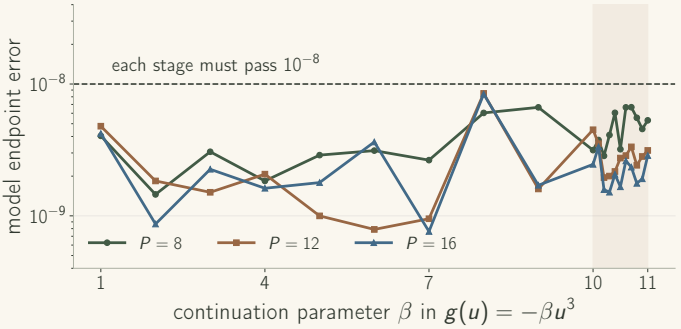
Continuation for the Focusing Cubic



Warm-start the harder problem. Solve $g(u) = -\beta u^3$ at a smaller β, then reuse that control at the next value.

Use steps of 1 up to $\beta = 10$, then 0.1 up to 11.

Continuation for the Focusing Cubic



Warm-start the harder problem. Solve $g(u) = -\beta u^3$ at a smaller β, then reuse that control at the next value.

Use steps of 1 up to $\beta = 10$, then 0.1 up to 11.

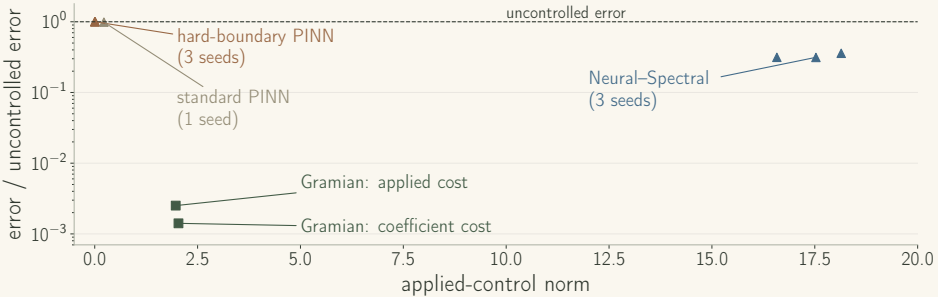
Observed result:

Newton–HUM passes at $P = 8, 12, 16$.

Continuation reaches the focusing benchmark numerically: each accepted stage meets the endpoint tolerance.

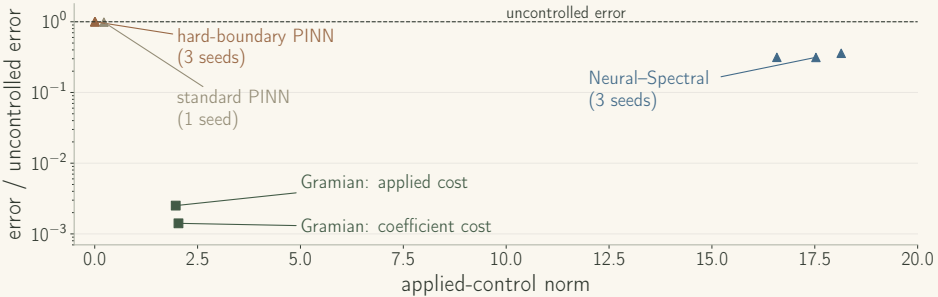
Two-Dimensional Accuracy and Control Effort

Linear square-domain test: 4×4 model modes, 8×8 check, $T = 7$. Read lower-left points as smaller endpoint error and less applied effort.



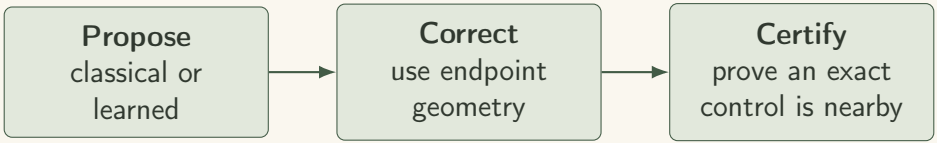
Two-Dimensional Accuracy and Control Effort

Linear square-domain test: 4×4 model modes, 8×8 check, $T = 7$. Read lower-left points as smaller endpoint error and less applied effort.



The spectral network improves the learned results; Gramian controls are much more accurate and use less effort here.

Conclusions and Discussion



- **Propose:** use a classical solver or a learned spectral control.
- **Correct:** use HUM endpoint sensitivities to reduce the nonlinear endpoint error.
- **Certify:** verify ε, γ, and L to locate an exact P-mode control near the computation.

Thank you.

Backup index | Precise hypotheses | Reuse and damping | References

Backup: Index

Theory

- Newton–HUM: precise hypotheses
- Source freezing in the energy space
- Combined response bound for the full PDE
- Scalar damping and local stability

Neural, metrics, references

- Approximation and error certification
- Approximation of a full-PDE steering pair
- Gramian reuse / control norms
- References 2 3 4

Newton–HUM Convergence: Precise Hypotheses

Let $\mathfrak{F}_P \colon \mathcal{U}_P \to \mathbb{R}^{2P}$ be C^1 on a ball of radius ρ around c_0, with

$$\|D\mathfrak{F}_P(v) - D\mathfrak{F}_P(w)\| \le L\,\|v - w\|\,, \qquad D\mathfrak{F}_P(v)R_v = I, \quad \|R_v\| \le \gamma$$

throughout that ball. Put $\varepsilon_0 = \|\mathfrak{F}_P(c_0)\|$ and

$$\theta = \frac{1}{2}L\gamma^2\varepsilon_0 < 1, \qquad \frac{\gamma\varepsilon_0}{1-\theta} < \rho.$$

Then the full-step iteration stays in the ball and

$$\varepsilon_{n+1} \le \frac{1}{2}L\gamma^2\varepsilon_n^2, \qquad \|c_{n+1} - c_n\| \le \gamma\varepsilon_n.$$

The certificate needs an inverse at one candidate; quadratic convergence needs a uniform inverse bound on the neighborhood.

Source Freezing in the Continuous Energy Space

Under GCC, let $\mathcal{H}_T$ solve the affine steering problem and suppose

$$\|\mathcal{H}_T(h_1) - \mathcal{H}_T(h_2)\|_{C\left([0,T];\mathcal{E}\right)} \leq C_T^{\mathrm{aff}} \, \|h_1 - h_2\|_{L^2(0,T;\mathcal{E})} \, .$$

If applying g to the state defines a globally Lipschitz map $g\colon H_0^1(\Omega) \to L^2(\Omega)$ with constant $L_g^{\mathcal{E}}$, then

$$q_\infty = C_T^{\mathrm{aff}} \sqrt{T} \, L_g^{\mathcal{E}} < 1$$

implies global contraction of the corresponding continuous source-frozen map.

Scope matters

The P-mode response constant $\chi_{P,T}$ comes from a different minimization problem. Its validated bound does not certify the full-PDE constant or prove a bound valid for every P.

A Combined Response Bound for the Full PDE

Assume GCC and a scalar Lipschitz constant ℓ_g for g. On $\mathcal{Z}_\infty := L^2\big(0,T;L^2(\Omega)\big)$, define

$$\mathscr{H}_{\infty,T}h = \pi_1(\mathcal{H}_T((0,h)) - \mathcal{H}_T((0,0)))\,,$$
$$\chi_{\infty,T} := \|\mathscr{H}_{\infty,T}\|_{\mathcal{L}(\mathcal{Z}_\infty)}\,.$$

Here π_1 selects displacement. The fixed endpoint data cancel.

Continuous contraction criterion

If $\widehat{q}_\infty := \ell_g \chi_{\infty,T} < 1$, the displacement map $\widehat{\mathcal{T}}_\infty(u) := \pi_1 \mathcal{H}_T((0,g(u)))$ has a unique fixed point u^* and

$$\|u-u^*\|_{\mathcal{Z}_\infty} \le \frac{\left\|u-\widehat{\mathcal{T}}_\infty(u)\right\|_{\mathcal{Z}_\infty}}{1-\widehat{q}_\infty}.$$

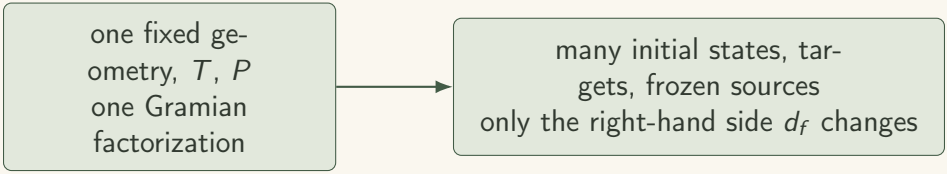
This is a full-PDE theorem under a smallness condition. We do not numerically enclose $\chi_{\infty,T}$.

Gramian Reuse for Different Control Problems

For the affine equation $y' = Ay + Bc + f$, the control with the smallest coefficient norm is

$$c_f(t) = B^\top e^{A^\top (T-t)} W_T^{-1} d_f,$$

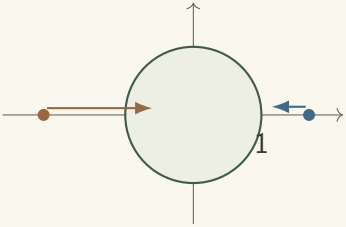
$$W_T = \int_0^T e^{A(T-s)} B B^\top e^{A^\top (T-s)} \, \mathrm{d}s.$$



$P = 16$, $\beta = 8$: all 64 control problems meet the relative error tolerance $E_T < 10^{-2} E_{\mathrm{free}}$; median $E_T = 3.1456 \times 10^{-7}$. Numerical reuse test: a different error tolerance, outside the proven contraction range.

Scalar Damping and Local Stability

$$a^{(n+1)} = (1-\eta)a^{(n)} + \eta \mathcal{T}_P\left(a^{(n)}\right), \qquad \lambda \longmapsto 1 + \eta(\lambda - 1).$$



eigenvalue diagram

For the Jacobian of the time-discretized iteration J, a positive scalar damping exists exactly when

$$\operatorname{Re}\lambda < 1 \quad \text{for all } \lambda \in \sigma(J).$$

Allowed step sizes satisfy

$$0 < \eta < \min_{\lambda \in \sigma(J)} \frac{2(1 - \operatorname{Re}\lambda)}{|\lambda - 1|^2}.$$

Neural Approximation and Error Certification

1. **Approximation at fixed model size.** Networks with bounded, nonconstant C^2 activation functions (such as tanh) approximate state coefficients in $H^2(0, T; \mathbb{R}^P)$ and controls in $L^2(0, T; \mathbb{R}^P)$.
2. **Solution error bounds.** The equation error over time and the initial mismatch bound the error relative to the separately solved P-mode system.
3. **Certification near an exact control.** For the P-mode system, if the endpoint derivative has a right inverse and is locally Lipschitz, sufficiently accurate nearby neural controls satisfy the certificate conditions.

These approximation and stability statements do not guarantee that Adam or L-BFGS finds a sufficiently accurate control.

Neural Approximation of a Full-PDE Steering Pair

On $\Omega = (0,1)$, take a mild steering pair with $\Phi^* \in C\big([0,T];\mathcal{E}\big)$ and $f^* \in L^2\big((0,T)\times\omega\big)$. Every displacement coefficient belongs to $H^2(0,T)$; extend f^* by zero outside ω. Use bounded, nonconstant C^2 activations.

Increase both spatial resolution and network width

For every $\varepsilon > 0$, some P, finite width W, and parameters θ give

$$\sup_{0\le t\le T}\left\|\Phi^*(t) - \widetilde{\Phi}_\theta(t)\right\|_{\mathcal{E}} < \varepsilon,$$

$$\left\|f^* - \mathbf{1}_\omega \widetilde{f}_\theta\right\|_{L^2\left((0,T)\times(0,1)\right)} < \varepsilon.$$

This proves what networks can represent, not what training finds or what a finite-model certificate proves about the PDE.

Control-Coefficient and Applied-Control Norms

$$\|c\|^2_{\text{modal}} = \int_0^T c^\top c \, \mathrm{d}t,$$

$$\|\mathbf{1}_\omega f_P\|^2_{L^2\left((0,T)\times\Omega\right)} = \int_0^T c^\top M_P c \, \mathrm{d}t.$$

Both 2D weighted Gramian controls have model endpoint errors below 2×10^{-10}:

Minimized cost	coefficient norm	applied norm	check $E_{8\times 8}$
$R = I$ (modal)	**2.103**	2.035	4.00×10^{-3}
$R = M$ (physical)	2.622	**1.968**	7.12×10^{-3}

Each weighting minimizes its own cost. Smaller effort need not mean smaller truncation error.

References: History and Applications

J. C. Maxwell (1868). On governors. Proc. R. Soc. London 16, 270–283.

D. M. Bošković and M. Krstić (2003). Stabilization of a solid propellant rocket instability by state feedback. Int. J. Robust Nonlinear Control 13, 483–495.

Okinawa Institute of Science and Technology (6 January 2025). OIST mathematicians develop new math to forecast natural phenomena and detect early cancer development. News report.

U. G. Abdulla and J. H. Rodrigues (2026). Cancer detection via electrical impedance tomography and optimal control of elliptic PDEs. Mathematics in Engineering 8(2), 308–339.

References: Wave Controllability

J.-L. Lions (1988). Contrôlabilité exacte, perturbations et stabilisation de systèmes distribués, Tome 1. Masson.

C. Bardos, G. Lebeau, and J. Rauch (1992). Sharp sufficient conditions for the observation, control, and stabilization of waves from the boundary. SIAM J. Control Optim. 30, 1024–1065.

E. Zuazua (1993). Exact controllability for semilinear wave equations in one space dimension. Ann. Inst. H. Poincaré C 10, 109–129.

B. Dehman and G. Lebeau (2009). Analysis of the HUM control operator and exact controllability for semilinear waves in uniform time. SIAM J. Control Optim. 48(2), 521–550.

S. Ervedoza and E. Zuazua (2012). The wave equation: control and numerics. In Control and Stabilization of Partial Differential Equations, Lecture Notes in Mathematics 2048, 245–339. Springer.

References: Constructive and Learning-Based Methods

A. Münch and E. Trélat (2022). Constructive exact control of semilinear 1D wave equations by a least-squares approach. SIAM J. Control Optim. 60, 652–673.

S. Claret, J. Lemoine, and A. Münch (2024). On the exact boundary controllability of semilinear wave equations. SIAM J. Control Optim. 62, 1953–1976.

S. Mowlavi and S. Nabi (2023). Optimal control of PDEs using physics-informed neural networks. J. Comput. Phys. 473, 111731.

Y. Du, N. Chalapathi, and A. S. Krishnapriyan (2024). Neural spectral methods: self-supervised learning in the spectral domain. ICLR.

M. Feng, Z. Chen, Y. Huang, Y. Liu, and J. Yan (2025). Optimal control operator perspective and a neural adaptive spectral method. AAAI 39(14), 14567–14575.

References: Validated Numerics

S. M. Rump (2010). Verification methods: rigorous results using floating-point arithmetic. Acta Numerica 19, 287–449.

W. Tucker (2011). Validated Numerics. Princeton University Press.

A. Hungria, J.-P. Lessard, and J. D. Mireles James (2016). Rigorous numerics for analytic solutions of differential equations: the radii polynomial approach. Math. Comp. 85, 1427–1459.